

## Crossover between High and Low Energy-States in Two-Coupled Chains of Tomonaga Model

Masahisa TSUCHIIZU, Hideo YOSHIOKA and Yoshikazu SUZUMURA

*Department of Physics, Nagoya University, Nagoya 464-01*

(Received July 22, 1997)

By applying the renormalization group method to two-coupled chains in the Tomonaga model, the role of interchain hopping has been studied in the entire energy region. The energy for a crossover from the perturbational regime to the relevant regime becomes smaller than that of the interchain hopping due to one-dimensional fluctuations of the mutual interaction. From the calculation of response functions for charge density waves and superconducting states, the phase diagram of dominant and subdominant states has been obtained in the plane of mutual interactions with fixed energy.

### §1. Introduction

Organic conductors,<sup>1)</sup> which exhibit low dimensional fluctuations, have been studied by using the model of quasi-one-dimensional systems, where the role of the interchain hopping plays an important role.

As a basic model for such a system, two-coupled chains of interacting electrons has been explored. Even in the simple case of spinless fermions described by the Tomonaga model, there exist significant properties involved in connecting a one-dimensional system with quasi-one dimensional system.<sup>2)–7)</sup> The ground state has been calculated in the limit of low energy. The relevant behavior of the interchain hopping leads to a state which differs essentially from that in the absence of hopping. Although the limiting state for the two-coupled chains of the Tomonaga model is well known, it is not yet clear how the state at finite temperature (or energy) is determined in the presence of both the interchain hopping and the mutual interactions.

The phase diagram in the plane of the intrachain interaction ( $g_2$ ) and the interchain interaction ( $g'_2$ ) is shown in Fig. 1(a) (Fig. 1(b)).<sup>7)</sup> This represents the result in the absence (presence) of the interchain hopping. In Fig. 1(a), there are two kinds of dominant states with in-phase pairing and out-of-phase pairing which are degenerate due to the absence of interchain hopping. Such a state corresponds to the state in the high energy limit, where the effect of the interchain hopping can be disregarded. The state in Fig. 1(b) is obtained in the limit of zero energy (or temperature). The interchain hopping plays a crucial role in the sense that the degeneracy for in-phase and out-of-phase pairings is removed and the other pairing state becomes subdominant due to the relevance of the interchain hopping. The subdominant state which is shown in the parenthesis could become meaningful for more complicated models, e.g., a model with a Fermi surface which exhibits an incomplete nesting condition in the case  $|g_2| > |g'_2|$ . Thus, it is of interest to examine the state with finite energy, which is expected to exhibit a phase diagram between Figs. 1(a) and (b).

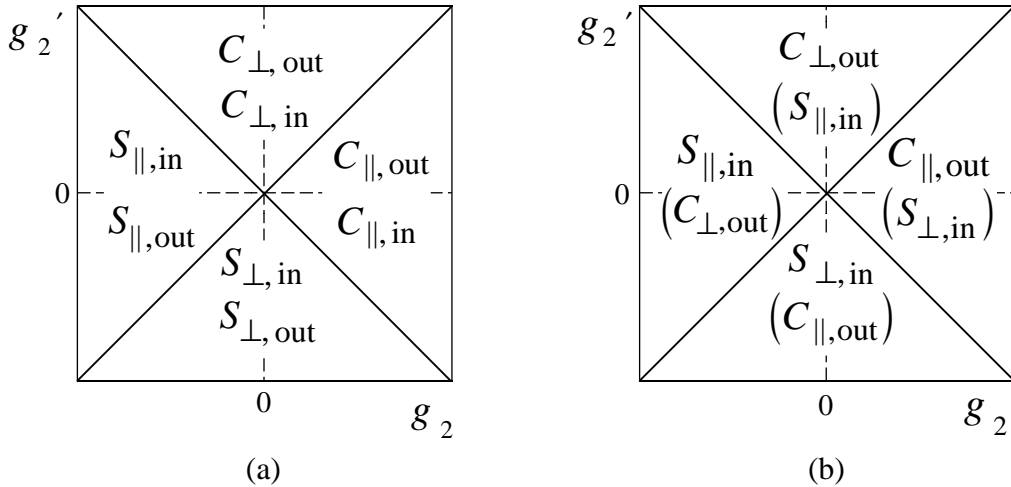


Fig. 1. Phase diagram in the plane of  $g_2 = \gamma_2/(2\pi v_F)$  and  $g_2' = \gamma_2'/(2\pi v_F)$  for  $t = 0$  (a) and  $t \neq 0$  (b),<sup>7)</sup> where  $C$  and  $S$  denote the CDW and SC state, respectively, and  $\parallel$  ( $\perp$ ) and out (in) denote the pairing state for the intrachain (interchain) and out of phase (in phase) ordering. For  $t = 0$  (a), there are two kinds of states as the dominant states, while for  $t \neq 0$  (b), the subdominant state is distinguished, as is shown in the parenthesis.

In deriving Fig. 1(b), it has been assumed that one-dimensional behavior vanishes and the relevant behavior of the interchain hopping begins when the energy (or temperature) becomes smaller than the hopping energy. In a quasi-one dimensional system, Bourbonnais<sup>8)</sup> has maintained that one-dimensional fluctuations still exist at temperatures lower than the hopping energy and that the temperature for the crossover becomes smaller than the hopping energy due to the suppression of the density of state around the Fermi energy.<sup>9)</sup> There is no explicit calculation which shows the reduction of the crossover temperature, even for two-coupled chains.

In the present paper, we study these problems in two-coupled chains of the Tomonaga model by applying the renormalization group method to the bosonized Hamiltonian. In §2, the Hamiltonian and possible order parameters are represented in terms of the phase variables. The scaling equations for coupling constants and response functions are given in §3. In §4, a phase diagram with a fixed energy is examined, and the crossover energy is evaluated as a function of mutual interactions. Section 5 is devoted to summary and discussion.

## §2. Model and order parameter

We consider two-coupled chains of the Tomonaga model, where a one-dimensional chain consists of spinless fermions with intrachain forward scattering, interchain forward scattering, and interchain hopping. The Hamiltonian with a chain of length  $L$  is given as

$$\mathcal{H} = \sum_{p,i} \int dx \psi_{p,i}^\dagger(x) v_F (-ip\partial_x - k_F) \psi_{p,i}(x)$$

$$\begin{aligned}
& -t \sum_p \int dx \left\{ \psi_{p,1}^\dagger(x) \psi_{p,2}(x) + \text{h.c.} \right\} \\
& + \frac{\gamma_2}{2} \sum_{p,i} \int dx \psi_{p,i}^\dagger(x) \psi_{-p,i}^\dagger(x) \psi_{-p,i}(x) \psi_{p,i}(x) \\
& + \frac{\gamma_2'}{2} \sum_p \int dx \left\{ \psi_{p,1}^\dagger(x) \psi_{-p,2}^\dagger(x) \psi_{-p,2}(x) \psi_{p,1}(x) + \text{h.c.} \right\}, \quad (2.1)
\end{aligned}$$

where  $\psi_{p,i}^\dagger$  is the fermion creation operator. The sign  $p = + (-)$  expresses the right (left) moving state, and  $i = 1 (2)$  denotes the indices of the chain, where  $v_F$  and  $k_F$  are the Fermi velocity and the Fermi wave vector, respectively. We consider the case in which the energy of interchain hopping,  $t$ , is much smaller than the Fermi energy,  $v_F k_F$ , and the matrix element of the intrachain (interchain) forward scattering,  $\gamma_2$  ( $\gamma_2'$ ), is smaller than  $2\pi v_F$ .

In Eq. (2.1) the first and second terms can be diagonalized by use of the transformation

$$\psi_{p,\sigma}(x) = (-\sigma \psi_{p,1}(x) + \psi_{p,2}(x)) / \sqrt{2}. \quad (2.2)$$

The index  $\sigma = \pm$  denotes that for the diagonalized band, where the new Fermi wave vector is given by  $k_{F\sigma} = k_F - \sigma t / v_F$  for the  $\sigma$ -band. By applying the bosonization method to the respective band, Eq. (2.1) is rewritten in terms of the phase Hamiltonian as  $\mathcal{H} = \mathcal{H}_\theta + \mathcal{H}_\phi$ ,<sup>6),7)</sup> where

$$\begin{aligned}
\mathcal{H}_\theta &= \frac{u}{4\pi} \int dx \left\{ \frac{1}{K_\theta} (\partial_x \theta_+)^2 + K_\theta (\partial_x \theta_-)^2 \right\}, \quad (2.3) \\
\mathcal{H}_\phi &= \frac{v_F}{4\pi} \int dx \left\{ \frac{1}{K_\phi} (\partial_x \phi_+)^2 + K_\phi (\partial_x \phi_-)^2 \right\} \\
&+ \frac{v_F}{2\pi\alpha^2} \int dx \left\{ g_{2\phi_+} \cos \left( 2\phi_+ - \frac{4t}{v_F} x \right) + g_{2\phi_-} \cos (2\phi_-) \right\}. \quad (2.4)
\end{aligned}$$

Equations (2.3) and (2.4) express the Hamiltonian of the total fluctuation and that of the transverse fluctuation, respectively, where  $u = v_F \sqrt{1 - (g_2 + g_2')^2}$ ,  $K_\theta = \sqrt{\{1 - (g_2 + g_2')\} / \{1 + (g_2 + g_2')\}}$ ,  $K_\phi = 1$ ,  $g_{2\phi_+} = -(g_2 - g_2')$ ,  $g_{2\phi_-} = g_2 - g_2'$  and  $\gamma_2 = 2\pi v_F g_2$  ( $\gamma_2' = 2\pi v_F g_2'$ ). The quantity  $\alpha^{-1}$ , which is of the order of  $k_F$ , is the cutoff for large wave vectors. The phase variables  $\theta_\pm$  and  $\phi_\pm$  in Eqs. (2.3) and (2.4) are defined as

$$\theta_\pm(x) = - \sum_{q \neq 0} \frac{\pi i}{qL} e^{-\frac{\alpha}{2}|q| + iqx} \sum_{k,\sigma} \left( a_{k,+,\sigma}^\dagger a_{k+q,+,\sigma} \pm a_{k,-,\sigma}^\dagger a_{k+q,-,\sigma} \right), \quad (2.5)$$

$$\phi_\pm(x) = - \sum_{q \neq 0} \frac{\pi i}{qL} e^{-\frac{\alpha}{2}|q| + iqx} \sum_{k,\sigma} \sigma \left( a_{k,+,\sigma}^\dagger a_{k+q,+,\sigma} \pm a_{k,-,\sigma}^\dagger a_{k+q,-,\sigma} \right), \quad (2.6)$$

where  $a_{k,p,\sigma} = (1/\sqrt{L}) \int dx e^{-ikx} \psi_{p,\sigma}(x)$ . By use of Eqs. (2.5) and (2.6), the field operator  $\psi_{p,\sigma}(x)$  is expressed as<sup>10)</sup>

$$\psi_{p,\sigma}(x) = \frac{1}{\sqrt{2\pi\alpha}} \exp[ipk_{F\sigma}x + p\Theta_{p,\sigma} + i\pi\Xi_{p,\sigma}] = \psi'_{p,\sigma}(x) \exp[i\pi\Xi_{p,\sigma}], \quad (2.7)$$

where  $\Theta_{p,\sigma} = i[\theta_+ + p\theta_- + \sigma(\phi_+ + p\phi_-)]/2$ . The phase factor  $i\pi\Xi_{p,\sigma}$ , which is introduced for the fermion operator, is given by  $\Xi_{+,+} = 0$ ,  $\Xi_{+,-} = \hat{N}_{+,+}$ ,  $\Xi_{-,+} = \hat{N}_{+,+} + \hat{N}_{+,-}$  and  $\Xi_{-,-} = \hat{N}_{+,+} + \hat{N}_{+,-} + \hat{N}_{-,+}$ , where  $\hat{N}_{p,\sigma} = \int dx \psi_{p,\sigma}^\dagger(x) \psi_{p,\sigma}(x)$  is the number operator for the fermion.

We examine the state with order parameters for the charge density wave (CDW) state and the superconducting (SC) state. In terms of phase variables, order parameters corresponding to Fig. 1(a) are expressed as follows.

(I) Order parameters for CDW with intrachain and out of (in) phase pairing are given by

$$\begin{aligned} \begin{pmatrix} C_{||,\text{out}} \\ C_{||,\text{in}} \end{pmatrix} &= \begin{pmatrix} \psi_{p,1}^\dagger \psi_{-p,1} - \psi_{p,2}^\dagger \psi_{-p,2} \\ \psi_{p,1}^\dagger \psi_{-p,1} + \psi_{p,2}^\dagger \psi_{-p,2} \end{pmatrix} = \begin{pmatrix} -\sum_{\sigma} \psi_{p,\sigma}^\dagger \psi_{-p,-\sigma} \\ \sum_{\sigma} \psi_{p,\sigma}^\dagger \psi_{-p,\sigma} \end{pmatrix} \\ &\rightarrow \begin{pmatrix} \sum_{\sigma} \sigma \psi_{p,\sigma}^\dagger \psi'_{-p,-\sigma} \\ \sum_{\sigma} \psi_{p,\sigma}^\dagger \psi'_{-p,\sigma} \end{pmatrix} \\ &= \frac{e^{-i2pk_{\text{F}}x}}{\pi\alpha} e^{-ip\theta_+} \begin{pmatrix} -i \sin \phi_- \\ \cos \left( \phi_+ - \frac{2t}{v_{\text{F}}} x \right) \end{pmatrix}. \end{aligned} \quad (2.8)$$

(II) Order parameters for CDW with interchain and out of (in) phase pairing are given by

$$\begin{aligned} \begin{pmatrix} C_{\perp,\text{out}} \\ C_{\perp,\text{in}} \end{pmatrix} &= \begin{pmatrix} \psi_{p,1}^\dagger \psi_{-p,2} - \psi_{p,2}^\dagger \psi_{-p,1} \\ \psi_{p,1}^\dagger \psi_{-p,2} + \psi_{p,2}^\dagger \psi_{-p,1} \end{pmatrix} = \begin{pmatrix} -\sum_{\sigma} \sigma \psi_{p,\sigma}^\dagger \psi_{-p,-\sigma} \\ -\sum_{\sigma} \sigma \psi_{p,\sigma}^\dagger \psi_{-p,\sigma} \end{pmatrix} \\ &\rightarrow \begin{pmatrix} \sum_{\sigma} \psi_{p,\sigma}^\dagger \psi'_{-p,-\sigma} \\ \sum_{\sigma} \sigma \psi_{p,\sigma}^\dagger \psi'_{-p,\sigma} \end{pmatrix} \\ &= \frac{e^{-i2pk_{\text{F}}x}}{\pi\alpha} e^{-ip\theta_+} \begin{pmatrix} \cos \phi_- \\ -ip \sin \left( \phi_+ - \frac{2t}{v_{\text{F}}} x \right) \end{pmatrix}. \end{aligned} \quad (2.9)$$

(III) Order parameters for the superconducting state with intrachain and in (out of) phase pairing are given by

$$\begin{aligned} \begin{pmatrix} S_{||,\text{in}} \\ S_{||,\text{out}} \end{pmatrix} &= \begin{pmatrix} \psi_{p,1} \psi_{-p,1} + \psi_{p,2} \psi_{-p,2} \\ \psi_{p,1} \psi_{-p,1} - \psi_{p,2} \psi_{-p,2} \end{pmatrix} = \begin{pmatrix} \sum_{\sigma} \psi_{p,\sigma} \psi_{-p,\sigma} \\ -\sum_{\sigma} \psi_{p,\sigma} \psi_{-p,-\sigma} \end{pmatrix} \\ &\rightarrow \begin{pmatrix} \sum_{\sigma} \psi'_{p,\sigma} \psi'_{-p,\sigma} \\ \sum_{\sigma} \sigma \psi'_{p,\sigma} \psi'_{-p,-\sigma} \end{pmatrix} \end{aligned}$$

$$= \frac{1}{\pi\alpha} e^{-ip\theta_-} \begin{pmatrix} \cos \phi_- \\ ip \sin \left( \phi_+ - \frac{2t}{v_F} x \right) \end{pmatrix}. \quad (2.10)$$

(IV) Order parameters for the superconducting state with interchain and in (out of) phase pairing are given by

$$\begin{aligned} \begin{pmatrix} S_{\perp, \text{in}} \\ S_{\perp, \text{out}} \end{pmatrix} &= \begin{pmatrix} \psi_{p,1} \psi_{-p,2} + \psi_{p,2} \psi_{-p,1} \\ \psi_{p,1} \psi_{-p,2} - \psi_{p,2} \psi_{-p,1} \end{pmatrix} = \begin{pmatrix} -\sum_{\sigma} \sigma \psi_{p,\sigma} \psi_{-p,\sigma} \\ -\sum_{\sigma} \sigma \psi_{p,\sigma} \psi_{-p,-\sigma} \end{pmatrix} \\ &\rightarrow \begin{pmatrix} \sum_{\sigma} \sigma \psi'_{p,\sigma} \psi'_{-p,\sigma} \\ \sum_{\sigma} \psi'_{p,\sigma} \psi'_{-p,-\sigma} \end{pmatrix} \\ &= \frac{1}{\pi\alpha} e^{-ip\theta_-} \begin{pmatrix} i \sin \phi_- \\ \cos \left( \phi_+ - \frac{2t}{v_F} x \right) \end{pmatrix}. \end{aligned} \quad (2.11)$$

The symbol  $\parallel$  ( $\perp$ ) represents the pairing in the chain (between two chains), and the symbol in (out) denotes pairing with the same (opposite) sign. The right arrow in the second line of Eqs. (2.8)~(2.11) denotes the process obtained from Eq. (2.7), where a numerical factor with absolute value of unity is discarded. In Eq. (2.4) and Eqs. (2.8)~(2.11), the quantity  $N_{+,+} - N_{-,+}$  is taken as an even integer, where  $N_{p,\sigma}$  is an eigenvalue of  $\hat{N}_{p,\sigma}$ . We note that the symmetry of the interactions is associated with the four kinds of order parameters of Eqs. (2.8)~(2.11). Since a quarter of the  $g_2$ - $g'_2$  plane in Fig. 1(a) is sufficient to understand all the states, we precisely examine the states in the region  $g_2 > |g'_2|$ .

### §3. Renormalization group method

Several kinds of order parameters introduced in the previous section are examined by calculating the response functions given by

$$\begin{aligned} R_A(x, \tau) &= \langle T_{\tau} A^{\dagger}(x, \tau) A(0, 0) \rangle \cdot 2(\pi\alpha)^2 \\ &= R_A^{\theta}(x, \tau) \cdot R_A^{\phi}(x, \tau), \end{aligned} \quad (3.1)$$

where  $A$  is the operator given by Eqs. (2.8)~(2.11). From Eq. (2.3),  $R_A^{\theta}(x, \tau)$  is calculated straightforwardly as

$$R_A^{\theta}(x, \tau) = \langle T_{\tau} e^{i\theta_{\pm}(x, \tau)} e^{-i\theta_{\pm}(0, 0)} \rangle = \left( \frac{\alpha}{\sqrt{x^2 + (v_F \tau)^2}} \right)^{K_{\theta}^{\pm 1}}, \quad (3.2)$$

where the sign  $+$  ( $-$ ) corresponds to the CDW (SC) state. Note that Eq. (3.2) depends only on  $r (= \sqrt{x^2 + (v_F \tau)^2})$ . From Eqs. (2.8)~(2.11), the quantity  $R_A^{\phi}(x, \tau)$  corresponding to the  $\phi$ -field is expressed as

$$R_A^{\phi}(x, \tau) = \overline{R_A^{\phi}(x, \tau)} \cdot f_A(x), \quad (3.3)$$

where

$$\overline{R}_A^\phi(x, \tau) = \begin{cases} R_{\sin \phi_-} \equiv 2 \langle T_\tau \sin \phi_-(x, \tau) \sin \phi_-(0, 0) \rangle & \text{for } A = C_{\parallel, \text{out}}, S_{\perp, \text{in}}, \\ R_{\cos \phi_-} \equiv 2 \langle T_\tau \cos \phi_-(x, \tau) \cos \phi_-(0, 0) \rangle & \text{for } A = C_{\perp, \text{out}}, S_{\parallel, \text{in}}, \\ R_{\sin \phi_+} \equiv \frac{2 \langle T_\tau \sin(\phi_+(x, \tau) + 2tx/v_F) \sin \phi_+(0, 0) \rangle}{\cos(2tx/v_F)} & \text{for } A = C_{\perp, \text{in}}, S_{\parallel, \text{out}}, \\ R_{\cos \phi_+} \equiv \frac{2 \langle T_\tau \cos(\phi_+(x, \tau) + 2tx/v_F) \cos \phi_+(0, 0) \rangle}{\cos(2tx/v_F)} & \text{for } A = C_{\parallel, \text{in}}, S_{\perp, \text{out}} \end{cases} \quad (3.4)$$

and the factor  $f_A(x)$  is defined as  $f_A(x) \equiv e^{i2pk_F x}$  for  $A = C_{\parallel, \text{out}}$  and  $C_{\perp, \text{out}}$ ,  $f_A(x) \equiv e^{i2pk_F x} \cos(2tx/v_F)$  for  $A = C_{\parallel, \text{in}}$  and  $C_{\perp, \text{in}}$ ,  $f_A(x) \equiv 1$  for  $A = S_{\parallel, \text{in}}$  and  $S_{\perp, \text{in}}$ , and  $f_A(x) \equiv \cos(2tx/v_F)$  for  $A = S_{\parallel, \text{out}}$  and  $S_{\perp, \text{out}}$ .

By using the renormalization group method with the assumption of invariance with respect to  $\alpha \rightarrow \alpha' = \alpha e^{dl}$ , response functions for the  $\phi_{\pm}$ -field are derived as (Appendix A)

$$\begin{aligned} R_{\sin \phi_-}(r) &= 2 \langle T_\tau \sin \phi_-(x, \tau) \sin \phi_-(0, 0) \rangle \\ &= \exp \left[ - \int_0^{\ln(r/\alpha)} \frac{1}{K_\phi(l)} dl \right] \cdot \exp \left[ + \int_0^{\ln(r/\alpha)} g_{2\phi_-}(l) dl \right], \end{aligned} \quad (3.5)$$

$$\begin{aligned} R_{\cos \phi_-}(r) &= 2 \langle T_\tau \cos \phi_-(x, \tau) \cos \phi_-(0, 0) \rangle \\ &= \exp \left[ - \int_0^{\ln(r/\alpha)} \frac{1}{K_\phi(l)} dl \right] \cdot \exp \left[ - \int_0^{\ln(r/\alpha)} g_{2\phi_-}(l) dl \right], \end{aligned} \quad (3.6)$$

$$\begin{aligned} R_{\sin \phi_+}(r) &= 2 \left\langle T_\tau \sin \left( \phi_+(x, \tau) - \frac{2t}{v_F} x \right) \sin \phi_+(0, 0) \right\rangle / \cos \left( \frac{2t}{v_F} x \right) \\ &= \exp \left[ - \int_0^{\ln(r/\alpha)} K_\phi(l) dl \right] \cdot \exp \left[ + \int_0^{\ln(r/\alpha)} g_{2\phi_+}(l) dl \right], \end{aligned} \quad (3.7)$$

$$\begin{aligned} R_{\cos \phi_+}(r) &= 2 \left\langle T_\tau \cos \left( \phi_+(x, \tau) - \frac{2t}{v_F} x \right) \cos \phi_+(0, 0) \right\rangle / \cos \left( \frac{2t}{v_F} x \right) \\ &= \exp \left[ - \int_0^{\ln(r/\alpha)} K_\phi(l) dl \right] \cdot \exp \left[ - \int_0^{\ln(r/\alpha)} g_{2\phi_+}(l) dl \right], \end{aligned} \quad (3.8)$$

where the term with the quantity  $\tan^{-1}(v_F \tau/x)$  has been neglected for the present numerical calculation with small  $t$ . In Eqs. (3.5)~(3.8), the quantities  $K_\phi(l)$ ,  $g_{2\phi_-}(l)$  and  $g_{2\phi_+}(l)$  are calculated from the renormalization equations,

$$\frac{d}{dl} K_\phi(l) = -\frac{1}{2} g_{2\phi_+}^2(l) K_\phi^2(l) J_0 \left( \frac{4t(l)}{v_F \alpha^{-1}} \right) + \frac{1}{2} g_{2\phi_-}^2(l), \quad (3.9)$$

$$\frac{d}{dl} g_{2\phi_+}(l) = (2 - 2K_\phi(l)) g_{2\phi_+}(l), \quad (3.10)$$

$$\frac{d}{dl} g_{2\phi-}(l) = (2 - 2/K_\phi(l)) g_{2\phi-}(l), \quad (3.11)$$

$$\frac{d}{dl} \left( \frac{4t(l)}{v_F \alpha^{-1}} \right) = \frac{4t(l)}{v_F \alpha^{-1}} - g_{2\phi+}^2(l) K_\phi(l) J_1 \left( \frac{4t(l)}{v_F \alpha^{-1}} \right), \quad (3.12)$$

where  $J_\nu(z)$  is the  $\nu$ -th Bessel function. Equations (3.5)~(3.12) have been derived by use of a method similar to that of Giamarchi and Schulz.<sup>11), 12)</sup> The initial conditions in Eqs. (3.9)~(3.12) are chosen as  $K_\phi(0) = 1$ ,  $g_{2\phi+}(0) = -(g_2 - g_2')$ ,  $g_{2\phi-}(0) = g_2 - g_2'$  and  $t(0) = t$ . We note that the renormalization equation (3.12) for small  $t$  becomes equal to that derived from the perturbation in terms of  $t$ .<sup>5)</sup> The negative sign of the second term of Eq. (3.12)<sup>13)</sup> indicates the reduction of interchain hopping.

From Eqs. (3.2), (3.5)~(3.8), the response function can be expressed as

$$\overline{R}_A(r) = R_A^\theta(x, \tau) \overline{R}_A^\phi(x, \tau), \quad (3.13)$$

where the largest response function and the next one in  $\overline{R}_A(r)$  with fixed length  $r (= \sqrt{x^2 + (v_F \tau)^2})$  (i.e., the corresponding energy  $v_F/r$ ) lead to the phase diagram for the dominant state and subdominant state, respectively.

In the present paper, we assume that the response function  $R_A(r)$  is equivalent to that of the Fourier transform with  $\omega = v_F/r$ . The validity of such a treatment is discussed in §5.

#### §4. Response functions and phase diagram

We examine the renormalization group equations given by Eqs. (3.9)~(3.12), where parameters are chosen as  $t/(v_F \alpha^{-1}) = 0.0025$  and  $g_2 - g_2' = 0.02$ . The  $l$ -dependence of  $K_\phi(l)$ ,  $g_{2\phi-}(l)$  and  $g_{2\phi+}(l)$  are shown in Fig. 2. Increasing  $l$ ,  $K_\phi(l)$  and  $g_{2\phi-}(l)$  increases to the strong coupling regime, while  $g_{2\phi+}(l)$  reduces to zero. Note that the quantities  $d(l)$  of Eq. (A.8), which is obtained by substituting the results of Eqs. (3.9)~(3.12), is invisible in the scale of Fig. 2. The actual variation of  $g_{2\phi-}(l)$  and  $g_{2\phi+}(l)$  appears for  $l \gtrsim \ln[v_F \alpha^{-1}/4t] \sim 4.6$ , which is designated by the arrow. This result indicates the validity of the previous treatment<sup>7)</sup> that  $K_\phi$  and  $g_{2\phi\pm}$  have been replaced by the initial values for  $e^l < v_F \alpha^{-1}/t$ . Since the Bessel function  $J_0(4t(l)/(v_F \alpha^{-1}))$  becomes small for  $e^l > v_F \alpha^{-1}/t$ , the  $\phi_+$ -term can be

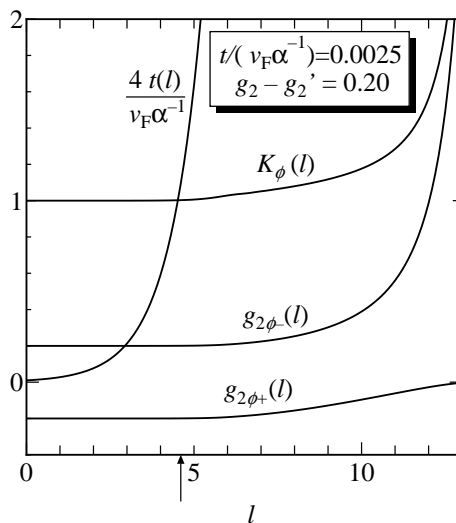


Fig. 2. Quantities  $K_\phi(l)$ ,  $g_{2\phi-}(l)$ ,  $g_{2\phi+}(l)$  and  $4t(l)/(v_F \alpha^{-1})$  as functions of  $l = \ln(r/\alpha)$  for  $t/(v_F \alpha^{-1}) = 0.0025$  and  $g_2 - g_2' = 0.20$ . The arrow denotes  $l = l_0 = \ln[v_F \alpha^{-1}/4t] (\simeq 4.6)$ .

neglected and leads to strong coupling due to the  $\phi_-$ -term. Equation (3.12) reveals the fact that the hopping energy is reduced by the mutual interaction. Therefore the range for the one-dimensional regime is examined in detail.

In Fig. 3 the present results (solid curves) are compared with the previous ones (dotted curves), which were obtained by using initial conditions, such that the terms including  $t(l)$  are discarded in Eqs. (3.9) and (3.12) and for which  $K(l_0) = 1$  and  $g_{2\phi-}(l_0) = g_2 - g'_2$  with  $l_0 = \ln[v_F\alpha^{-1}/4t]$ .<sup>6,7)</sup> In the solid curve of  $K_\phi(l) - 1$ , the tangent, which displays the linear dependence for  $1 \lesssim l \lesssim 5$ , exhibits a rapid variation for  $l \simeq 6$ , indicating the crossover of the scaling property from the one-dimensional regime to the regime of relevant hopping. Therefore we define such a point,  $l = l_1$ , by the condition that the absolute value of the variation of the tangent becomes maximum. Good agreement between the solid curve and the dashed curve is obtained for  $l > l_1$ , where  $l_1 > \ln[v_F\alpha^{-1}/4t]$ . For the small  $l$  ( $\ll l_1$ ), Eqs. (3.9)~(3.11) up to the lowest order of  $t/(v_F\alpha^{-1})$  and  $g_2 - g'_2$  are calculated as (Appendix B)

$$K_\phi(l) = 1 + (g_2 - g'_2)^2 \left( \frac{t}{v_F\alpha^{-1}} \right)^2 (e^{2l} - 1) + \dots, \quad (4.1)$$

$$g_{2\phi+}(l) = -(g_2 - g'_2) + (g_2 - g'_2)^3 \left( \frac{t}{v_F\alpha^{-1}} \right)^2 (e^{2l} - 1 - 2l) + \dots, \quad (4.2)$$

$$g_{2\phi-}(l) = (g_2 - g'_2) + (g_2 - g'_2)^3 \left( \frac{t}{v_F\alpha^{-1}} \right)^2 (e^{2l} - 1 - 2l) + \dots. \quad (4.3)$$

Equations (4.1) and (4.3) can reproduce the numerical results sufficiently, i.e., the linear dependence of the solid curves for  $l < l_1$  in Fig. 3. Thus it turns out that there is a perturbational effect of  $t$  for the one-dimensional regime which is obtained for  $l < l_1$ . The dependence of the crossover energy on the interaction is discussed later.

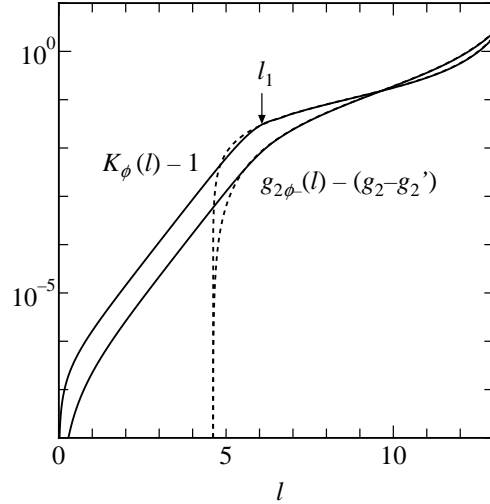


Fig. 3. The  $l$ -dependence of  $K_\phi(l) - 1$  and  $g_{2\phi-}(l) - (g_2 - g'_2)$ , which denote the variation from the initial values. The parameters are the same as in Fig. 2. The dotted curves represent the previous results,<sup>6)</sup> which were obtained by use of the initial condition that  $g_{2\phi+}(l_0) = 0$ ,  $K(l_0) = 1$  and  $g_{2\phi-}(l_0) = g_2 - g'_2$  with  $l_0 = \ln[v_F\alpha^{-1}/4t]$ . The factor 2 error in the renormalization equation of the previous papers<sup>6,7)</sup> is corrected. The quantity  $l_1$  denotes  $l$  for the onset for the relevant behavior of  $K_\phi(l)$  in the presence of  $t$ .



By substituting the solutions of Eqs. (3.9)~(3.12) into Eqs. (3.5)~(3.8), we obtain response functions for  $\phi_{\pm}$  which are shown by the solid curve in Fig. 4 for  $t/(v_F\alpha^{-1}) = 0.0025$  and  $g_2 - g'_2 = 0.2$ . The dotted line corresponds to those in the absence of the hopping. For  $\ln(r/\alpha) < l_1 (\simeq 6)$ , the response functions of  $R_{\sin\phi_-}(r)$  and  $R_{\cos\phi_+}(r)$  ( $R_{\cos\phi_-}(r)$  and  $R_{\sin\phi_+}(r)$ ) are almost the same as that for  $t = 0$  (dashed line), and their deviations from the dashed line due to the interchain hopping become visible for  $\ln(r/\alpha) > l_1$ . Since the renormalization group method is based on perturbation with respect to  $g_{2\phi+}$  and  $g_{2\phi-}$ , the present result is valid only for the regime of weak coupling. For large  $\ln(r/\alpha)$ ,  $R_{\sin\phi_-}(r)$  increases due to the strong coupling but is actually reduced to a finite value. We define  $l_3 (\equiv \ln(r_3/\alpha))$  as the location for the crossover from the weak coupling regime to the strong coupling regime which corresponds to a minimum of  $R_{\sin\phi_-}(r)$ . As is shown in Appendix C, the excitation gap,  $\Delta$ , in Eq. (2.4) can be estimated from  $\Delta = v_F\alpha^{-1} \exp[-l_{\Delta}]$  with  $2(K_{\phi}(l_{\Delta}) - 1) \simeq 1$ , i.e.,

$$\Delta = 4t \exp \left[ -\frac{\pi}{2} \frac{1}{|g_2 - g'_2|} + 1 \right]. \quad (4.4)$$

In the inset in Fig. 4,  $\ln R_{\sin\phi_-}(r_3)$  (solid curve) as a function of  $1/(g_2 - g'_2)$  is compared with the analytical function  $R_{\sin\phi_-}(r_{\Delta})$  (dash-dotted curve) where  $l_{\Delta} \equiv \ln(r_{\Delta}/\alpha)$ . Since  $r_3 \simeq r_{\Delta}$ , it is found that the minimum of  $R_{\sin\phi_-}(r)$  at  $r_3$  corresponds to the formation of the gap.

Now we examine the actual response function of Eq. (3.13), which is a product of the response function of the total fluctuation and that of the transverse one. In Fig. 5, the response functions with the largest (the dominant one), the second largest (the subdominant one) and the third largest in magnitudes are shown for  $t/v_F\alpha^{-1} = 0.0025$ ,  $g_2 - g'_2 = 0.20$  and  $g_2 + g'_2 = 0.10$ . In previous paper,<sup>6),7)</sup> the dominant and the subdominant states were examined in the limits of both long range (Fig. 1(b)) and  $t \rightarrow 0$ . In the present study, by tracking a state with arbitrary length scale (corresponding to the inverse of the energy) we found that the crossover of the second dominant states from  $C_{\parallel,\text{in}}$  to  $S_{\perp,\text{in}}$  occurs at  $\ln(r/\alpha) = l_2$ . In the region of

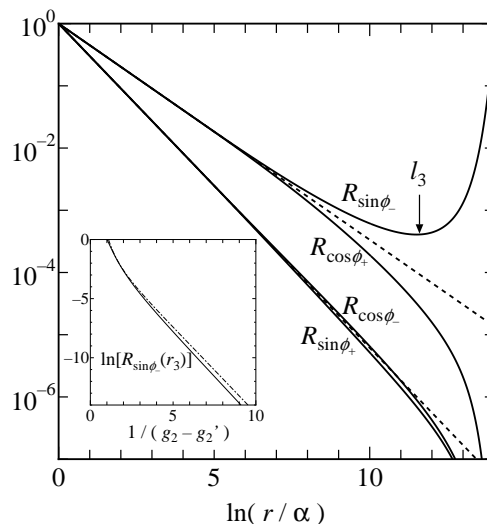


Fig. 4. The response functions of the  $\phi_{\pm}$ -field as a function of  $\ln(r/\alpha)$ , where  $r = \sqrt{x^2 + (v_F\tau)^2}$ . The quantities  $R_{\sin\phi_-}(r)$ ,  $R_{\cos\phi_+}(r)$ ,  $R_{\sin\phi_+}(r)$  and  $R_{\cos\phi_-}(r)$  are defined by Eqs. (3.5), (3.6), (3.7) and (3.8), respectively. The parameters are the same as in Fig. 2. The dotted lines denote the response functions with  $t = 0$ , and the location,  $l_3 (= \ln(r_3/\alpha))$ , corresponds to a minimum of  $R_{\sin\phi_-}(r)$ . In the inset,  $\ln[R_{\sin\phi_-}(r_3)]$  (solid curve) as a function of  $g_2 - g'_2$  is compared with the analytical one (the dash-dotted curve).

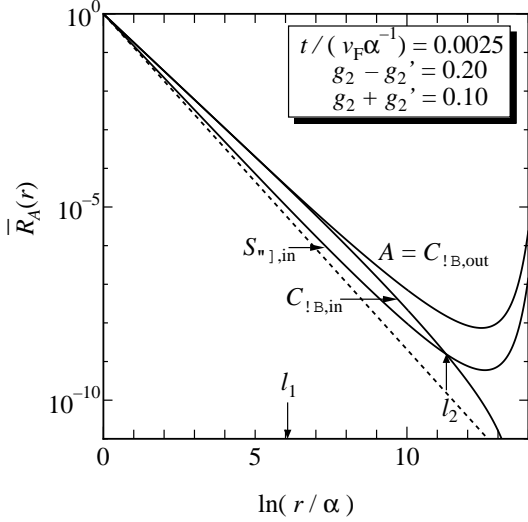


Fig. 5. The normalized response functions,  $\overline{R}_A(r)$ , of the order parameters,  $C_{\parallel,\text{out}}$ ,  $C_{\parallel,\text{in}}$  and  $S_{\perp,\text{in}}$  as functions of  $\ln(r/\alpha)$ , where  $t/(v_F\alpha^{-1}) = 0.0025$ ,  $g_2 - g_2' = 0.20$ ,  $g_2 + g_2' = 0.10$  and notation is the same as in Fig. 1. The dotted line denotes the response function in the absence of interactions. With increasing  $\ln(r/\alpha)$ , the difference between  $C_{\parallel,\text{out}}$  and  $C_{\parallel,\text{in}}$  becomes notable for  $\ln(r/\alpha) > l_1$ , and a subdominant response function varies from  $C_{\parallel,\text{in}}$  to  $S_{\perp,\text{in}}$  at  $\ln(r/\alpha) = l_2$ .

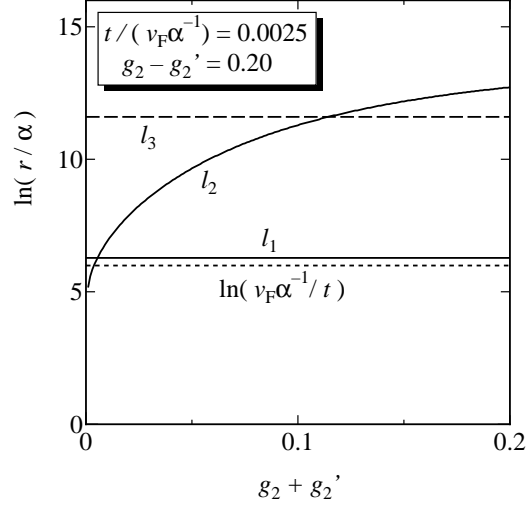


Fig. 6. Quantities  $l_1$  and  $l_2$  as functions of  $g_2 + g_2'$ , with fixed  $t/(v_F\alpha^{-1}) = 0.0025$  and  $g_2 - g_2' = 0.20$ , where the one-dimensional regime, i.e., the irrelevant  $t(l)$  is obtained for  $0 < \ln(r/\alpha) < l_1$  and the subdominant state is given by  $C_{\parallel,\text{in}}$  ( $S_{\perp,\text{in}}$ ) for  $\ln(r/\alpha) < l_2$  ( $\ln(r/\alpha) > l_2$ ). The value  $l_3$  (dashed line) is the upper bound for the present treatment of the renormalization group method. The maximum value for the one-dimensional regime denoted by  $l_1$  is larger than  $\ln[v_F\alpha^{-1}/4t]$  (dotted line).

$\ln(r/\alpha) < l_1$ , there is still a small effect of the interchain hopping which removes the degeneracy of  $C_{\perp,\text{out}}$  and  $C_{\parallel,\text{in}}$ . Such an effect can be seen analytically: Eq. (3-13) with  $\ln(r/\alpha) \ll l_1$  is expanded as

$$\overline{R}_{C_{\parallel,\text{out}}}(r) = \left(\frac{\alpha}{r}\right)^{K_\theta} \left(\frac{\alpha}{r}\right)^{1-(g_2-g_2')} \times \left[ 1 + \frac{(g_2 - g_2')^2}{32} \left(\frac{4t(0)}{v_F\alpha^{-1}}\right)^2 \left\{ e^{2\ln(r/\alpha)} - 1 - 2\ln\left(\frac{r}{\alpha}\right) \right\} + \dots \right], \quad (4-5)$$

$$\overline{R}_{C_{\parallel,\text{in}}}(r) = \left(\frac{\alpha}{r}\right)^{K_\theta} \left(\frac{\alpha}{r}\right)^{1-(g_2-g_2')} \times \left[ 1 - \frac{(g_2 - g_2')^2}{32} \left(\frac{4t(0)}{v_F\alpha^{-1}}\right)^2 \left\{ e^{2\ln(r/\alpha)} - 1 - 2\ln\left(\frac{r}{\alpha}\right) \right\} + \dots \right], \quad (4-6)$$

$$\overline{R}_{S_{\perp,\text{in}}}(r) = \left(\frac{\alpha}{r}\right)^{1/K_\theta} \left(\frac{\alpha}{r}\right)^{1-(g_2-g_2')} \times \left[ 1 + \frac{(g_2 - g_2')^2}{32} \left(\frac{4t(0)}{v_F\alpha^{-1}}\right)^2 \left\{ e^{2\ln(r/\alpha)} - 1 - 2\ln\left(\frac{r}{\alpha}\right) \right\} + \dots \right]. \quad (4-7)$$

For the range satisfying  $\ln(r/\alpha) > l_3$  corresponding to an energy lower than  $\Delta$ , there appears a gap in the transverse fluctuation due to the relevance of the interchain hopping which leads to a large enhancement for  $C_{\parallel,\text{out}}$  and  $S_{\perp,\text{out}}$  and strong suppression for  $C_{\parallel,\text{in}}$ . We have found two kinds of quantities,  $l_1$  and  $l_2$ , where coupling constants are renormalized toward the relevant  $t$  in the region  $\ln(r/\alpha) > l_1$  and  $S_{\perp,\text{in}}$  is found as the subdominant state due to the relevant  $t$  in the region  $\ln(r/\alpha) > l_2$ . In Fig. 6,  $l_1$  and  $l_2$  are shown as a function of  $g_2 + g'_2$ . The dashed line denotes  $l_3$  corresponding to the upper bound of  $\ln(r/\alpha)$  for the present treatment of the renormalization group method and the dotted line denotes  $\ln[v_F\alpha^{-1}/t]$ . In the region with  $\ln(r/\alpha) < l_1$ , the state exhibits one-dimensional properties since the interchain hopping can be treated perturbatively. We note that  $l_2 < l_1$  for small  $g_2 + g'_2$  due to  $l_2 \simeq (g_2 + g'_2)(g_2 - g_2)^{-2}(v_F\alpha^{-1}/t)^2$  which is obtained from Eqs. (4.5), (4.7) and  $(g_2 + g'_2)l \ll 1$ .

Based on the results of Figs. 5 and 6, we obtain the phase diagram as a function of  $g_2$  and  $g'_2$  for the dominant and subdominant states with fixed  $\ln(r/\alpha)$ . The boundary between  $C_{\parallel,\text{in}}$  and  $S_{\perp,\text{in}}$  is obtained from Fig. 6 by estimating  $g_2$  and  $g'_2$  which satisfy  $\ln(r/\alpha) = l_2$  with fixed  $r$ . For example, the subdominant state,  $S_{\perp,\text{in}}$ , with  $\ln(r/\alpha) = 12$  appears in case  $g_2 - g'_2 = 0.20$  and  $g_2 + g'_2 < 0.11$  due to the enhancement of the charge fluctuation. We note that the response function with fixed  $r$  corresponds to the response function for finite energy with  $\omega = v_F/r$ . In Fig. 7, the phase diagram in the  $g_2$ - $g'_2$  plane is shown with  $t/(v_F\alpha^{-1}) = 0.0025$  and fixed  $\ln(r/\alpha) = 12$ . The solid line denotes the boundary for the dominant state and the dotted line is the boundary for the subdominant state. The results of Figs. 5 and 6 correspond to the state in the region  $g_2 > |g'_2|$ , i.e.,  $I_L$  and  $I_H$ , which show the states with low energy and high energy, respectively. The phase diagram of the entire region has been obtained by use of the symmetry property of order parameters which is given by Eqs. (2.8)~(2.11). The region of  $J_L$  ( $J = I, II, III$  and  $IV$ ) which is similar to the state in the zero limit of energy decreases rapidly by the decrease of  $\ln(r/\alpha)$ . We have found that the region of  $J_L$  becomes very narrow in case  $\ln(r/\alpha) \simeq l_1$  ( $\simeq \ln[v_F\alpha^{-1}/t]$ ). Therefore the phase diagram is similar to Fig. 1(a) for most of the region in the  $g_2$ - $g'_2$  plane in the case that  $\ln(r/\alpha) < l_1$ , i.e., for energy larger than  $t$ .

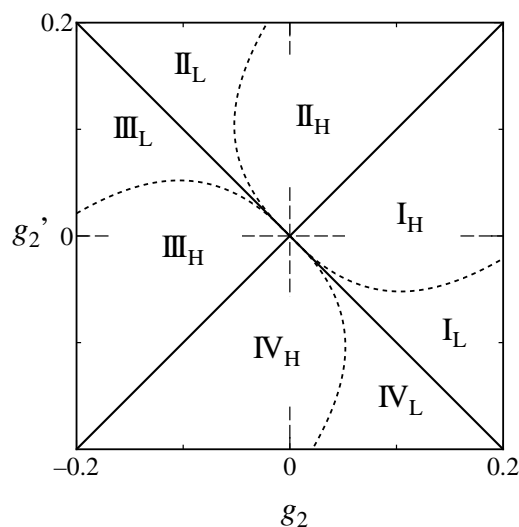


Fig. 7. Phase diagram for several kinds of order parameters in the plane of  $g_2$  and  $g'_2$ , where the dominant states (subdominant states) are given by  $C_{\parallel,\text{out}}$  ( $S_{\perp,\text{in}}$ ),  $C_{\parallel,\text{out}}$  ( $C_{\parallel,\text{in}}$ ),  $C_{\perp,\text{out}}$  ( $S_{\parallel,\text{in}}$ ),  $C_{\perp,\text{out}}$  ( $C_{\perp,\text{in}}$ ),  $S_{\parallel,\text{in}}$  ( $C_{\perp,\text{out}}$ ),  $S_{\parallel,\text{in}}$  ( $S_{\parallel,\text{out}}$ ) and  $S_{\perp,\text{in}}$  ( $C_{\parallel,\text{out}}$ ),  $S_{\perp,\text{in}}$  ( $S_{\perp,\text{out}}$ ) for the regions  $I_L$ ,  $I_H$ ,  $II_L$ ,  $II_H$ ,  $III_L$ ,  $III_H$  and  $IV_L$ ,  $IV_H$ , respectively. The dotted curve, which corresponds to the boundary for the subdominant states is calculated for  $\ln(r/\alpha) = \ln(v_F\alpha^{-1}/\omega) = 12$ .

Finally we examine the characteristic energy  $\omega_1$  which separates the one-dimensional regime from the relevant regime of  $t$ . The length corresponding to  $\omega_1$  is shown by  $l_1 = \ln[v_F\alpha^{-1}/\omega_1]$  in Fig. 3. In Fig. 8 the quantity  $\omega_1/t$  is shown as a function of  $t/(v_F\alpha^{-1})$  with fixed  $g_2 - g'_2 = 0.1, 0.2, 0.3$  and  $0.4$ . The quantity  $\omega_1/t$  decreases by the increase of  $g_2 - g'_2$  and increases with increasing  $t/(v_F\alpha^{-1})$ . The dotted line which is obtained by use of the extrapolation of the solid curve is expressed as  $\omega_1/t = \text{const} \cdot [t/(v_F\alpha^{-1})]^{\alpha_1}$ , where  $\alpha_1$  depends on  $g_2 - g'_2$ . Such a characteristic energy  $\omega_1$  can be estimated from Eq. (3.12) by assuming that  $\omega_1 \simeq \omega'_1 = v_F\alpha^{-1} \exp[-l'_1]$  with  $t(l'_1)/(v_F\alpha^{-1}) = O(1)$ , where  $l'_1 \simeq l_1$ . Since Eq. (3.12) is calculated as  $t(l)/(v_F\alpha^{-1}) = t/(v_F\alpha^{-1}) \exp\{1 - (g_2 - g'_2)^2/2\}l$  for  $t/(v_F\alpha^{-1}) \ll 1$ , we obtain

$$\omega'_1 = \text{const} \cdot t \left( t / \{v_F\alpha^{-1}\} \right)^{(g_2 - g'_2)^2/2}. \quad (4.8)$$

In the inset of Fig. 8,  $\alpha_1$  obtained from the data of the solid curve is represented by the closed circle which is compared with the  $\alpha_1 = (g_2 - g'_2)^2/2$  of Eq. (4.8) (dash-dotted curve). The good agreement of the two results indicates the validity of Eq. (4.8) as a characteristic energy  $\omega_1$ . Here we note the assertion of Bourbonnais<sup>8)</sup> that one-dimensional fluctuation does exist at temperatures lower than the energy of the transverse hopping  $t_\perp$  in quasi-one-dimensional systems. The suppression of the crossover temperature  $T_x$  ( $< t_\perp$ ) in a quasi-one-dimensional system comes from the reduction of the density of states at the Fermi energy, which is caused by the mutual interaction.<sup>9)</sup> We find that  $\omega_1$  of the present calculation is essentially the same as  $T_x$  since a system of two-coupled chains already shares common features with a quasi-one-dimensional system regarding the role of interchain hopping.

## §5. Summary and discussion

In the present paper, we have examined the role of interchain hopping in the entire energy region in two-coupled chains of the Tomonaga model by use of the renormalization group method. From the calculation of response functions for CDW and SC states in the real space, we obtained the phase diagram in the plane of mutual interactions in which the dominant and subdominant states are shown with fixed energy or temperature. The interchain hopping exhibits a perturbational effect for energy higher than  $\omega_1$  ( $= v_F\alpha^{-1} e^{-l_1}$ ), while the degeneracy of in-phase and out-

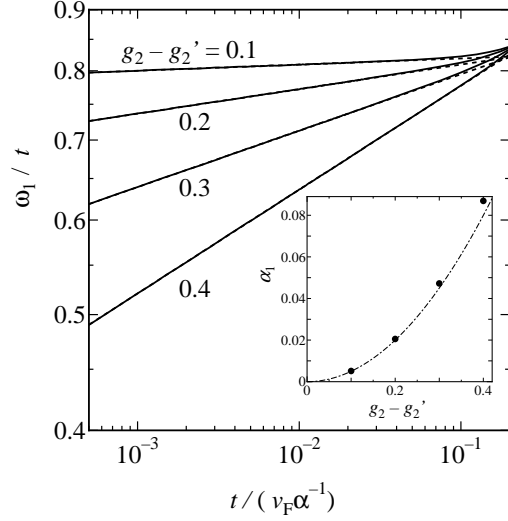


Fig. 8. The ratio of  $\omega_1$  to  $t$  as a function of  $t/(v_F\alpha^{-1})$ , where  $\omega_1 \equiv v_F\alpha^{-1} \exp[-l_1]$ . The dotted line is the extrapolation which is given by using the equation  $\omega_1/t \propto (t/v_F\alpha^{-1})^{\alpha_1}$ . In the inset,  $\alpha_1$  is shown as a function of  $g_2 - g'_2$ , where the dash-dotted curve denotes  $\alpha_1 = (1/2)(g_2 - g'_2)^2$ .

of-phase parings is removed due to the relevant behavior of the hopping for energy lower than  $\omega_1$ . The hopping leads to the formation of the excitation gap in the transverse fluctuation of the  $\phi$ -field for energy lower than  $v_F\alpha^{-1}e^{-l_3}$ . The crossover energy,  $\omega_1$ , is lower than  $t$  due to the interaction which gives rise to the reduction of the density of states at the Fermi surface.

We have examined the two-chain system by use of the renormalization group method in real space in order to examine the states at finite energy or at finite temperature. We comment on the relation between the present result and that derived by the scaling of the energy cutoff, i.e., in Fourier space. Fabrizio<sup>14)</sup> has studied the same model by applying the renormalization group method with the scaling of energy to Eq. (2.1), where *all* interactions are calculated perturbatively. In the present calculation, the two-chain system is transformed into the phase Hamiltonian through the bosonization method, where only the non-linear terms  $g_{2\phi-}$  and  $g_{2\phi+}$  are treated perturbatively. By replacing  $l(= \ln(\alpha'/\alpha))$  with  $-\ln(\omega'_0/\omega_0)$ , where  $\omega_0(\sim v_F/\alpha)$  is the band cutoff, it is found that the renormalization equations of the coupling constants obtained by Fabrizio are the same as ours, Eqs. (3.9)~(3.12), up to the lowest order of the coupling constants and the interchain hopping. But there is a difference in the terms of higher order in the interchain hopping. Invariance of the renormalization equations with respect to  $t \rightarrow -t$  exists in the present result, Eq. (3.12), but does not for his results. It is not yet clear if such a discrepancy comes from the present choice of the phase Hamiltonian or from some other source.

Finally, we discuss the response functions at finite energy. Since, to our knowledge, there is no calculation for response functions of two-coupled chains in terms of the renormalization group method with an energy cutoff, we mention the case of no misfit parameter, i.e., a one-dimensional Fermi gas. The response function for the energy cutoff is calculated by applying the renormalization group method to the quantity given by  $\bar{R}_i(0, \omega) = \pi v_F(\partial R_i(0, \omega)/\partial \ln \omega)$ ,<sup>15)</sup> where  $R_i(k, \omega)$  is the Fourier transform of  $R_i(r)$ . By comparing Eqs. (3.5)~(3.8) in the case  $t = 0$ <sup>12)</sup> with  $\bar{R}_i(0, \omega)$ ,<sup>15)</sup> it turns out that  $R_i(r)/(\alpha/r)^2$  with  $r/\alpha = \omega_0/\omega$  can be replaced by  $\bar{R}_i(0, \omega)$  when the  $l$ -dependences of  $K_\phi(l)$  and  $g_{2\phi\pm}(l)$  are neglected. In the present calculation, such a replacement is justified for  $l \lesssim 10$  and is meaningful qualitatively for larger  $l$ . Thus, the present results may correspond to those at finite energy or at finite temperature.

### Acknowledgements

This work was partially supported by a Grant-in-Aid for Scientific Research (09640429) from the Ministry of Education, Science, Sports and Culture.

### Appendix A

#### — Derivation of Renormalization Equations —

The response functions are calculated by use of the renormalization group method as follows.<sup>11)</sup> Treating the nonlinear terms in Eq. (2.4), i.e.,  $g_{2\phi+-}$  and  $g_{2\phi-}$ -terms, as the perturbation, the response function for  $R_{\sin\phi-}(x, \tau)$  of Eq. (3.5) up to the

second order is calculated as

$$\begin{aligned}
R_{\sin \phi_-}(x_1 - x_2, \tau_1 - \tau_2) &= 2 \langle T_\tau \sin \phi_-(x_1, \tau_1) \sin \phi_-(x_2, \tau_2) \rangle \\
&= \exp \left[ -\frac{1}{K_\phi} U(r_1 - r_2) \right] \\
&\times \left[ 1 + \frac{1}{4\pi} g_{2\phi^-} e^{(2/K_\phi)U(r_1-r_2)} \int \frac{d^2 r_3}{\alpha^2} e^{-(2/K_\phi)U(r_1-r_3)} e^{-(2/K_\phi)U(r_2-r_3)} \right. \\
&\quad - \frac{1}{2} g_{2\phi^+}^2 \int \frac{dr}{\alpha} \left( \frac{r}{\alpha} \right)^{3-4K_\phi} J_0 \left( \frac{4t}{v_F} r \right) U(r_1 - r_2) \\
&\quad - \frac{1}{4} g_{2\phi^+}^2 \int \frac{dr}{\alpha} \left( \frac{r}{\alpha} \right)^{3-4K_\phi} J_2 \left( \frac{4t}{v_F} r \right) \cos 2\theta_{r_1-r_2} \\
&\quad \left. + \frac{1}{2} g_{2\phi^-}^2 \frac{1}{K_\phi^2} \int \frac{dr}{\alpha} \left( \frac{r}{\alpha} \right)^{3-4/K_\phi} U(r_1 - r_2) + \dots \right], \tag{A.1}
\end{aligned}$$

where  $r = \sqrt{x^2 + (v_F \tau)^2}$ ,  $U(r) = \ln(r/\alpha)$  and  $\tan \theta_r = v_F \tau / x$ .  $J_\nu(z)$  is the  $\nu$ -th Bessel function. By raising the expansion of r.h.s. of Eq. (A.1) to the exponential and using  $\alpha$  as the lower cutoff of the integrations, one obtains

$$\begin{aligned}
R_{\sin \phi_-}(x_1 - x_2, \tau_1 - \tau_2) &= \exp \left[ -\frac{1}{K_\phi^{\text{eff}}} U(r_1 - r_2) - d^{\text{eff}} \cos(2\theta_{r_1-r_2}) \right] \\
&\times \left[ 1 + \frac{1}{4\pi} g_{2\phi^-} e^{(2/K_\phi)U(r_1-r_2)} \int_\alpha \frac{d^2 r_3}{\alpha^2} e^{-(2/K_\phi)U(r_1-r_3)} e^{-(2/K_\phi)U(r_2-r_3)} + \dots \right], \tag{A.2}
\end{aligned}$$

where the effective quantities are given by

$$\begin{aligned}
K_\phi^{\text{eff}} &= K_\phi - \frac{1}{2} g_{2\phi^+}^2 K_\phi^2 \int_\alpha \frac{dr}{\alpha} \left( \frac{r}{\alpha} \right)^{3-4K_\phi} J_0 \left( \frac{4t}{v_F} r \right) \\
&\quad + \frac{1}{2} g_{2\phi^-}^2 \int_\alpha \frac{dr}{\alpha} \left( \frac{r}{\alpha} \right)^{3-4/K_\phi}, \tag{A.3}
\end{aligned}$$

$$d^{\text{eff}} = d + \frac{1}{4} g_{2\phi^+}^2 K_\phi^2 \int_\alpha \frac{dr}{\alpha} \left( \frac{r}{\alpha} \right)^{3-4K_\phi} J_2 \left( \frac{4t}{v_F} r \right). \tag{A.4}$$

The parameter  $d$  is introduced in the zeroth order, where  $d = 0$  at  $l = 0$ . By assuming the scaling relations that Eqs. (A.3) and (A.4) are invariant for  $\alpha \rightarrow \alpha' = \alpha e^{dl}$ , the renormalization equations for the coupling constants are obtained as

$$\frac{d}{dl} K_\phi(l) = -\frac{1}{2} g_{2\phi^+}^2(l) K_\phi^2(l) J_0 \left( \frac{4t(l)}{v_F \alpha^{-1}} \right) + \frac{1}{2} g_{2\phi^-}^2(l), \tag{A.5}$$

$$\frac{d}{dl} g_{2\phi^+}(l) = (2 - 2K_\phi(l)) g_{2\phi^+}(l), \tag{A.6}$$

$$\frac{d}{dl}g_{2\phi-}(l) = (2 - 2/K_\phi(l)) g_{2\phi-}(l), \quad (\text{A}\cdot 7)$$

$$\frac{d}{dl}d(l) = \frac{1}{4}g_{2\phi+}^2(l) K_\phi^2(l) J_2\left(\frac{4t(l)}{v_F\alpha^{-1}}\right), \quad (\text{A}\cdot 8)$$

where  $\alpha(0) = \alpha$  in the Bessel functions. The renormalization for  $4t(l)/(v_F\alpha^{-1})$  is calculated as follows. The actual difference of the density between the two bands of Eq. (2.2),  $\Delta n$ , is given by

$$\Delta n = -2t\alpha/v_F + \frac{T}{L}\alpha \int dx d\tau \langle \partial_x \phi_+ \rangle, \quad (\text{A}\cdot 9)$$

where  $\partial_x \phi_+ = \pi \Sigma_p(\psi_{p,+}^\dagger \psi_{p,+} - \psi_{p,-}^\dagger \psi_{p,-})$ . The renormalization equation for  $t(l)$  is derived by assuming the scaling relation for Eq. (A.9). The second term on the r.h.s of Eq. (A.9) is rewritten as

$$\begin{aligned} \int dx d\tau \langle \partial_x \phi_+ \rangle &= \frac{1}{Z} \text{Tr} \left[ \int dx d\tau \partial_x \phi_+ e^{-\int d\tau \mathcal{H}} \right] \\ &= \frac{1}{Z} \text{Tr} \left[ \frac{\partial}{\partial \lambda} \exp \left\{ -\int d\tau \mathcal{H} + \lambda \int dx d\tau \partial_x \phi_+ \right\}_{\lambda=0} \right], \end{aligned} \quad (\text{A}\cdot 10)$$

where  $Z = \text{Tr} \exp[-\int d\tau \mathcal{H}]$ . By writing  $\tilde{\phi}_+ = \phi_+ - (2\pi/v_F)K_\phi \lambda x$  in Eq. (A.10), Eq. (A.9) is calculated as

$$\begin{aligned} \Delta n &= -\frac{2t}{v_F\alpha^{-1}} + \frac{2}{\alpha}g_{2\phi+}K_\phi \frac{T}{L} \int dx d\tau \left\langle x \sin \left( 2\phi_+ - \frac{4t}{v_F}x \right) \right\rangle \\ &= -\frac{2t}{v_F\alpha^{-1}} + \frac{1}{2}g_{2\phi+}^2K_\phi \int_\alpha^\infty \frac{dr}{\alpha} \left( \frac{r}{\alpha} \right)^{2-4K} J_1 \left( \frac{4t}{v_F}r \right) + \dots \end{aligned} \quad (\text{A}\cdot 11)$$

The infinitesimal transformation  $\alpha' = e^{dl}\alpha$  for Eq. (A.11) leads to

$$\frac{d}{dl} \left( \frac{4t(l)}{v_F\alpha^{-1}} \right) = \frac{4t(l)}{v_F\alpha^{-1}} - g_{2\phi+}^2(l) K_\phi(l) J_1 \left( \frac{4t(l)}{v_F\alpha^{-1}} \right). \quad (\text{A}\cdot 12)$$

Note that the present model is similar to but slightly different from the model of a single chain of fermions with spin 1/2.<sup>11)</sup> The hopping  $t$  corresponds to the external magnetic field in the latter model, where the renormalization equation for the magnetization has been derived by assuming that the external magnetic field satisfies the scaling relations.

The response functions are calculated by writing  $R_i(x, \tau) = F_i(r) \cdot \exp[-K_\phi^{\pm 1} \ln(r/\alpha) - d \cos 2\theta_r]$ , where  $i = \sin \phi_-, \cos \phi_-, \sin \phi_+$  and  $\cos \phi_+$  and the  $\pm$  sign corresponds the response function for the  $\phi_\pm$ -field. By assuming the scaling relation  $F_i(r, \alpha(l), K_\phi(l), g_{2\phi\pm}(l)) = I_i(dl, K_\phi(l), g_{2\phi\pm}(l)) \cdot F_i(r, \alpha(l+dl), K_\phi(l+dl), g_{2\phi\pm}(l+dl))$ , the multiplicative factor  $I_i$  for  $F_{\sin \phi_-}$  is obtained as

$$\begin{aligned} &I_{\sin \phi_-}(dl, K_\phi, g_{2\phi\pm}) \\ &= \exp \left[ g_{2\phi-} dl - \frac{1}{2}g_{2\phi+}^2 J_0 \left( \frac{4t}{v_F\alpha^{-1}} \right) U(r_1 - r_2) dl \right] \end{aligned}$$

$$\left. -\frac{1}{4}g_{2\phi+}^2 J_2 \left( \frac{4t}{v_F \alpha^{-1}} \right) \cos 2\theta_{r_1-r_2} dl + \frac{1}{2}g_{2\phi-}^2 \frac{1}{K_\phi^2} U(r_1 - r_2) dl \right]. \quad (\text{A}\cdot 13)$$

Thus the functions  $F_i$  are expressed as<sup>12)</sup>

$$F_i(r, K_\phi, g_{2\phi\pm}) = \exp \left[ \sum_{l=0}^{\ln(r/\alpha)} \ln[I_i(dl, K_\phi(l), g_{2\phi\pm}(l))] \right]. \quad (\text{A}\cdot 14)$$

Equations (A·12) (A·13) and (A·14) lead to

$$R_{\sin\phi-}(x, \tau) = \exp \left[ \int_0^{\ln(r/\alpha)} dl \left\{ -\frac{1}{K_\phi(l)} + g_{2\phi-}(l) \right\} - d \left( l = \ln \left( \frac{r}{\alpha} \right) \right) \cos 2\theta_r \right], \quad (\text{A}\cdot 15)$$

where other response functions are obtained in a similar way. We note that the last term of Eq. (A·15) is discarded in Eqs. (3·5)~(3·8), i.e.,  $R_A(r)$ , due to the condition  $d \ll 1$  in the present numerical calculation.

## Appendix B

— Derivation of Eqs. (4·1) ~ (4·3) —

We examine the renormalization equations for small  $l/l_1$ . Noting that  $4t(l)/(v_F \alpha^{-1}) \ll 1$  for the small  $l/l_1$ , we use the approximation that  $J_0(4t(l)/(v_F \alpha^{-1})) \simeq 1 - \{4t(l)/(v_F \alpha^{-1})\}^2/4$  and  $J_1(4t(l)/(v_F \alpha^{-1})) \simeq \{4t(l)/(v_F \alpha^{-1})\}/2$ . By retaining terms up to the order of  $(g_2 - g_2')^2$ , Eq. (3·12) is calculated as

$$\frac{4t(l)}{v_F \alpha^{-1}} = \tilde{t} \exp \left[ \left( 1 - \frac{g^2}{2} \right) l \right], \quad (\text{B}\cdot 1)$$

where  $\tilde{t} \equiv 4t/(v_F \alpha^{-1})$  and  $g \equiv g_2 - g_2'$ . By rewriting  $K_\phi(l)$  as  $K_\phi(l) = 1 + g_0(l)/2$  and making use of Eq. (B·1), Eqs. (3·9), (3·10) and (3·11) are calculated as

$$g_0(l) = \frac{\tilde{t}^2}{8} g^2 (e^{2l} - 1), \quad (\text{B}\cdot 2)$$

$$g_{2\phi+}(l) = -g + \frac{\tilde{t}^2}{16} g^3 (e^{2l} - 1 - 2l), \quad (\text{B}\cdot 3)$$

$$g_{2\phi-}(l) = g + \frac{\tilde{t}^2}{16} g^3 (e^{2l} - 1 - 2l), \quad (\text{B}\cdot 4)$$

which correspond to Eqs. (4·1), (4·2) and (4·3), respectively.

## Appendix C

— Estimation of the Energy Gap —

We examine Eqs. (3·9)~(3·12) with small coupling constants for  $l \gg l_1$ , where the term including  $J_\nu(4t(l)/(v_F \alpha^{-1}))$  and  $g_{2\phi+}$  can be disregarded. In this case, the



renormalization group equations are rewritten as

$$\frac{d}{dl}K_\phi(l) = \frac{1}{2}g_{2\phi-}^2(l), \quad (\text{C}\cdot 1)$$

$$\frac{d}{dl}g_{2\phi-}(l) = \left(2 - \frac{2}{K_\phi(l)}\right)g_{2\phi-}(l), \quad (\text{C}\cdot 2)$$

where the initial condition is given by  $K_\phi(l_0) = 1$  and  $g_{2\phi-}(l_0) = g_2 - g'_2$  with  $l_0 = -\ln[4t/(v_F\alpha^{-1})]$ . The differential equations (C·1) and (C·2) can be integrated as

$$\begin{aligned} g_{2\phi-}^2(l) - 8(K_\phi(l) - \ln K_\phi(l)) &= g_{2\phi-}^2(l_0) - 8(K_\phi(l_0) - \ln K_\phi(l_0)) \\ &\simeq g_{2\phi-}^2(l) - g_0^2(l) - 8 = (g_2 - g'_2)^2 - 8, \end{aligned} \quad (\text{C}\cdot 3)$$

where  $K_\phi(l) = 1 + g_0(l)/2$ . From Eqs. (C·1)~(C·3), one obtains

$$g_0(l) = |g_2 - g'_2| \tan [ |g_2 - g'_2|(l - l_0) ]. \quad (\text{C}\cdot 4)$$

By defining the gap  $\Delta$  as  $\Delta \equiv v_F\alpha^{-1} \exp[-l_\Delta]$  with  $g_0(l_\Delta) = 1$ , one obtains for  $\Delta$ ,

$$\Delta = 4t \exp \left[ -\frac{\pi}{2} \frac{1}{|g_2 - g'_2|} + 1 \right]. \quad (\text{C}\cdot 5)$$

From Eqs. (C·3)~(C·5) the response function  $R_{\sin\phi-}(r)$  at  $l_\Delta (= \ln(r_\Delta/\alpha))$  is calculated as

$$\begin{aligned} R_{\sin\phi-}(r_\Delta) &= \exp \left[ \int_0^{l_\Delta} dl \left( -\frac{1}{K_\phi(l)} + g_{2\phi-}(l) \right) \right] \\ &= \left( \frac{4t}{v_F\alpha^{-1}} \right)^{1-(g_2-g'_2)} \exp \left[ -\frac{\pi}{2} \frac{1}{|g_2 - g'_2|} + 1 \right] \\ &\quad \times \left( 1 + \frac{1}{(g_2 - g'_2)^2} \right)^{1/4} \left( \frac{1}{|g_2 - g'_2|} + \sqrt{1 + \frac{1}{(g_2 - g'_2)^2}} \right), \end{aligned} \quad (\text{C}\cdot 6)$$

which is shown as a function of  $1/(g_2 - g'_2)$  in the inset in Fig. 4.

### References

- [1] For Review, D. Jérôme and H. J. Schulz, *Adv. Phys.* **31** (1982), 299.  
T. Ishiguro and K. Yamaji, *Organic Superconductors*, Springer Series in Solid-State Sciences (Springer-Verlag, Berlin, 1990), Vol. 88.
- [2] X. G. Wen, *Phys. Rev.* **B42** (1990), 6623.
- [3] F. V. Kusmartsev, A. Luther and A. Nersesyan, *JETP Lett.* **55** (1992), 724.
- [4] V. M. Yakovenko, *JETP Lett.* **56** (1992), 510.
- [5] A. A. Nersesyan, A. Luther and F. V. Kusmartsev, *Phys. Lett.* **A176** (1993), 363.
- [6] H. Yoshioka and Y. Suzumura, *J. Phys. Soc. Jpn.* **63** (1994), 4298.
- [7] H. Yoshioka and Y. Suzumura, *J. Phys. Soc. Jpn.* **64** (1995), 3811.
- [8] C. Bourbonnais, *Mol. Cryst. Liq. Cryst.* **119** (1985), 11  
C. Bourbonnais and L. G. Caron, *Int. J. Mod. Phys.* **B5** (1991), 1033.
- [9] Y. Suzumura, *Prog. Theor. Phys.* **63** (1980), 51.
- [10] A. Luther and I. Peschel, *Phys. Rev.* **B9** (1974), 2911.

- [11] T. Giamarchi and H. J. Schulz, *J. de Phys.* **49** (1988), 819.
- [12] T. Giamarchi and H. J. Schulz, *Phys. Rev.* **B39** (1989), 4620.
- [13] There is an error of the the sign in the corresponding equation in the previous calculation.<sup>7)</sup>
- [14] M. Fabrizio, *Phys. Rev.* **B48** (1993), 15838.
- [15] J. Sólyom, *Adv. Phys.* **28** (1979), 201.